This article was downloaded by: [Renmin University of China]
On: 13 October 2013, At: 10:48
Publisher: Taylor & Francis
Informa Ltd Registered in England and Wales Registered Number: 1072954 Registered office: Mortimer House, 37-41 Mortimer Street, London W1T 3JH, UK

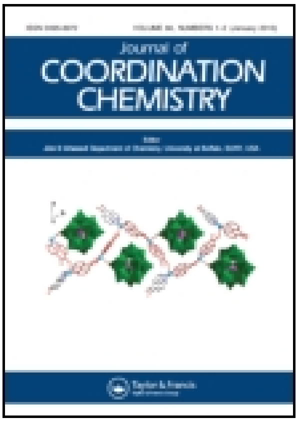

Journal of Coordination Chemistry
Publication details, including instructions for authors and subscription information:
http://www.tandfonline.com/loi/gcoo20

Synthesis, structural characterization, and properties of two new polyoxovanadates based on decavanadate $[V_{10}O_{28}]^{6-}$

Wentao Hou [a], Jiuyu Guo [a], Zuoxiang Wang [b] & Yan Xu [a]
[a] State Key Laboratory of Materials-Oriented Chemical Engineering, College of Chemistry and Chemical Engineering, Nanjing University of Technology, Nanjing, P.R. China
[b] School of Chemistry and Engineering, Southeast University, Nanjing, P.R. China

Published online: 20 Jun 2013.

To cite this article: Wentao Hou, Jiuyu Guo, Zuoxiang Wang & Yan Xu (2013) Synthesis, structural characterization, and properties of two new polyoxovanadates based on decavanadate $[V_{10}O_{28}]^{6-}$, Journal of Coordination Chemistry, 66:14, 2434-2443, DOI: 10.1080/00958972.2013.806986

To link to this article: http://dx.doi.org/10.1080/00958972.2013.806986

PLEASE SCROLL DOWN FOR ARTICLE

Taylor & Francis makes every effort to ensure the accuracy of all the information (the "Content") contained in the publications on our platform. However, Taylor & Francis, our agents, and our licensors make no representations or warranties whatsoever as to the accuracy, completeness, or suitability for any purpose of the Content. Any opinions and views expressed in this publication are the opinions and views of the authors, and are not the views of or endorsed by Taylor & Francis. The accuracy of the Content should not be relied upon and should be independently verified with primary sources of information. Taylor and Francis shall not be liable for any losses, actions, claims, proceedings, demands, costs, expenses, damages, and other liabilities whatsoever or howsoever caused arising directly or indirectly in connection with, in relation to or arising out of the use of the Content.

This article may be used for research, teaching, and private study purposes. Any substantial or systematic reproduction, redistribution, reselling, loan, sub-licensing, systematic supply, or distribution in any form to anyone is expressly forbidden. Terms &

Journal of Coordination Chemistry, 2013
Vol. 66, No. 14, 2434–2443, http://dx.doi.org/10.1080/00958972.2013.806986

Taylor & Francis
Taylor & Francis Group

Synthesis, structural characterization, and properties of two new polyoxovanadates based on decavanadate $[V_{10}O_{28}]^{6-}$

WENTAO HOU†, JIUYU GUO†, ZUOXIANG WANG‡ and YAN XU*†

†State Key Laboratory of Materials-Oriented Chemical Engineering, College of Chemistry and Chemical Engineering, Nanjing University of Technology, Nanjing, P.R. China
‡School of Chemistry and Engineering, Southeast University, Nanjing, P.R. China

(*Received 6 February 2013; in final form 27 March 2013*)

Two new decavanadate metal compounds, $[Co(pyim)_3]_2[V_{10}O_{28}]\cdot7H_2O$ (**1**) and $[Ni(pyim)_3]_2[H_2V_{10}O_{28}]\cdot4H_2O$ (**2**) (pyim = 2-(2-pyridyl)-imidazole), have been synthesized under hydrothermal conditions and characterized by elemental analysis, single-crystal X-ray diffraction analysis, infrared spectra, powder X-ray diffraction analysis, and thermogravimetric analysis. Crystallographic analysis reveals that **1** is constructed from $[V_{10}O_{28}]^{6-}$, metal cation $[Co(pyim)_3]^{3+}$, and water. $[V_{10}O_{28}]^{6-}$ clusters are connected by waters through O–H···O hydrogen bonds to form a sheet structure which is further connected by N–H···O hydrogen bonds to form a 3-D supermolecular framework. In **2**, although $[Ni(pyim)_3]^{2+}$ is similar to $[Co(pyim)_3]^{3+}$ in **1**, the M–O cluster anion is protonated $[H_2V_{10}O_{28}]^{4-}$.

Keywords: Hydrothermal synthesis; Polyoxovanadates; Organic–inorganic hybrid material; Crystal structure; Hydrogen bond

1. Introduction

Polyoxometalates (POMs) are significant because of their intriguing architectures [1–3] and potential applications in catalysis, medicine, biology, and materials science [4–8]. A hot research area in POM chemistry is to construct organic–inorganic hybrid materials by using POMs as inorganic building blocks, further linked by metal-organic units [9, 10]. In cage-like or sheet-like POMs in organic–inorganic hybrid materials, ligand usually bridges metal ions [11, 12]. As a branch of POMs, polyoxovanadates (POVs) play an important role in POM chemistry. V–O clusters exhibit a range of different dimensionality due to various polyhedral fragments built of VO_n units ($n = 4, 5, 6$) [13–15]. As there are diverse types of VO_4, VO_5, and VO_6 polyhedron building units, VO_n units can connect by edge-sharing, corner-sharing or surface-sharing to construct various V–O compounds, for instance, $[V_5O_{14}]^{3-}$ [16], $[V_{10}O_{26}]^{4-}$ [17], $[V_{10}O_{28}]^{6-}$ [18], $[V_{12}O_{32}]^{4-}$ [19], $[V_{13}O_{34}]^{4-}$ [20], $[V_{18}O_{42}]^{12-}$ [21], etc. POVs as discrete clusters, 1-D chains, 2-D sheets, or 3-D frameworks have been reported [22–24]. As an important member in POVs, different decavanadate compounds have been reported [25–32]. Decavanadate compounds are made of

---

*Corresponding author. Email: yanxu@njut.edu.cn

$[V_{10}O_{28}]^{6-}$ units; sometimes $[V_{10}O_{28}]^{6-}$ units can be protonated as $[HV_{10}O_{28}]^{5-}$, $[H_2V_{10}O_{28}]^{4-}$, $[H_3V_{10}O_{28}]^{3-}$, or $[H_4V_{10}O_{28}]^{2-}$ [30, 31]. To produce new compounds based on $[V_{10}O_{28}]^{6-}$, numerous approaches have been developed, such as controlling the synthetic route, temperature, mole ratio, pH, counter ion, etc. [33]. The counter ion associated to $[V_{10}O_{28}]^{6-}$ can be organic or inorganic cations, $[Na(H_2O)_8]_2H_2V_{10}O_{28}\cdot 4H_2O$ [34], $[NH_3(CH_2)_4NH_3][H_2pip]_2[V_{10}O_{28}]\cdot 6H_2O$ [35], and $K_2Zn_2V_{10}O_{28}\cdot 16H_2O$ [36]. Decavanadates with transition metal ions coordinated by large organic ligand have been less reported [25–29]. Organic ligands based on pyridyl imidazoles have not been reported in vanadate compounds. It is significant to design hybrid POVs with transition metals coordinated by pyridyl imidazoles to explore the mechanism of formation and the properties. In this article, we report two POV-based hybrid compounds, $[Co(pyim)_3]_2[V_{10}O_{28}]\cdot 7H_2O$ (**1**) and $[Ni(pyim)_3]_2[H_2V_{10}O_{28}]\cdot 4H_2O$ (**2**). The rigid bi-heterocyclic N-donors are connected by cobalt and nickel. Although the structure of $[Ni(pyim)_3]^{2+}$ is similar with $[Co(pyim)_3]^{3+}$ in **1**, the M–O cluster anion is protonated $[H_2V_{10}O_{28}]^{4-}$ in **2**.

2. Experimental

2.1. *Materials and physical techniques*

2-(2-Pyridyl)-imidazole was prepared according to literature methods [37], while other chemicals were of reagent grade obtained from commercial sources and used without purification. C, H, and N elemental analyses were performed on a Perkin-Elmer 2400 CHN elemental analyzer. Infrared spectra were recorded as KBr pellets on a Nicolet 410 FTIR spectrometer. TG analyses were carried out in nitrogen from 25 to 800 °C at a heating rate of 10 °C min^{-1} on a Diamond TG/DTA (Perkin-Elmer) thermal analyzer. Solid state luminescence properties were carried out using a F-4600 FL Spectrophotometer.

2.2. *Syntheses*

2.2.1. $[Co(pyim)_3]_2[V_{10}O_{28}]\cdot 7H_2O$. Both compounds were prepared by a solvothermal method. In a typical synthesis of **1**, a mixture of NH_4VO_3 (0.0747 g, 0.64 mM), $Co(CH_3CO_2)_2\cdot 4H_2O$ (0.1000 g, 0.4 mM), and 2-(2-pyridyl)-imidazole (0.0288 g, 0.2 mM) was added into a mixed solvent of 2 mL CH_3CH_2OH and 5 mL H_2O and stirred for 30 min. Then, the pH was adjusted to 6.0 with 2.0 M L^{-1} NaOH, and the solution was stirred for one more hour. Then, the resulting mixture was transferred into a 25 mL Teflon-lined stainless-steel autoclave and heated to 160 °C for 4 days. After cooling to room temperature, the product was washed with water and dried in air for 1 day to give orange rhombic crystals (0.0423 g, yield 32% based on V). Elemental analysis found (%): C, 28.78; H, 2.71; N, 12.27 (Calcd (%): C, 27.85; H, 2.63; N, 12.18).

2.2.2. $[Ni(pyim)_3]_2[H_2V_{10}O_{28}]\cdot 4H_2O$. The synthetic process of **2** was similar to **1**, but $Co(CH_3CO_2)_2\cdot 4H_2O$ was replaced by $Ni(CH_3CO_2)_2\cdot 4H_2O$ (0.1000 g, 0.4 mM). Orange rod crystals were obtained (0.0477 g, yield 37% based on V). Elemental analysis was found (%): C, 29.32; H, 2.67; N, 12.55 (Calcd (%): C, 28.54; H, 2.59; N, 12.48).

2.3. *X-ray crystallography*

The single crystals of **1** and **2** were glued onto a thin glass fiber by epoxy glue in air for data collection. Single-crystal XRD data were obtained from a Bruker Apex II CCD with Mo-Kα radiation ($\lambda = 0.71073$ Å) at 296 K using ω-2θ scan method. The crystal structures of **1** and **2** were solved by direct methods and refined by full-matrix least-squares methods on F^2 using SHELX97 program package [38]. All nonhydrogen atoms were refined anisotropically. Hydrogens of organic ligands were refined in calculated positions, assigned isotropic thermal parameters, and allowed to ride on their parent atoms. Further details of the crystal data and structure refinement are listed in table 1. Selected bond distances and angles are listed in tables S1 and S2.

3. Results and discussion

3.1. *Synthesis*

Many factors influence growth and structures of the crystals. Choosing appropriate solvent is crucial in such reactions. The pyim has higher solubility in ethanol than in water, while the other reactants are more soluble in water than in ethanol, so we use water and ethanol

Table 1. Crystal data and structure refinement for **1** and **2**.

Compound	**1**	**2**
Empirical formula	$C_{48}H_{54}Co_2N_{18}O_{35}V_{10}$	$C_{48}H_{52}N_{18}Ni_2O_{32}V_{10}$
Formula weight	2070.35	2019.90
Temperature (K)	296(2)	296(2)
Wavelength (Å)	0.71073	0.71073
Crystal system	Monoclinic	Triclinic
Space group	$P2_1/c$	$P2_1/c$
Unit cell dimensions (Å, °)		
a	10.9327(13)	13.2575(17)
b	24.113(3)	12.5556(16)
c	14.4257(17)	20.760(3)
α		
β	93.159	97.462(2)
γ		
Volume (Å^3)	3797.13(80)	3426.4(8)
Z	2	2
Calculated density (g/cm^3)	1.81068	1.958
Absorption coefficient (mm^{-1})	1.691	1.933
F(000)	2064	2016
Crystal size (mm^3)	0.16 × 0.13 × 0.12	0.17 × 0.16 × 0.13
Limiting indices	$-11 \leqslant h \leqslant 13; -28 \leqslant k \leqslant 28; -17 \leqslant l \leqslant 17$	$-15 \leqslant h \leqslant 15; -14 \leqslant k \leqslant 14; -24 \leqslant l \leqslant 24$
Reflections collected/unique	26,432/6680 [$R_{(int)} = 0.0626$]	23,839/6042 [$R_{(int)} = 0.0390$]
Max. and min. transmission	0.8229 and 0.7737	0.7872 and 0.7347
Refinement method	Full-matrix least-squares on F^2	Full-matrix least-squares on F^2
Data/parameters	6680/523	6042/511
Goodness-of-fit on F^2	1.097	1.057
Final *R* indices [$I > 2\sigma(I)$]	$R_1 = 0.0634$, $wR_2 = 0.2148$	$R_1 = 0.0409$, $wR_2 = 0.1036$
R indices (all data)	$R_1 = 0.1027$, $wR_2 = 0.2334$	$R_1 = 0.0564$, $wR_2 = 0.1096$

as mixed solvent to increase solubility. The pH is also important in the reactions. Parallel experiments showed that we can only obtain the two compounds when pH 6.0.

3.2. *Crystal structure*

The crystal structure of **1** contains two $[Co(pyim)_3]^{3+}$, one $[V_{10}O_{28}]^{6-}$, and water as shown in figure 1. The discrete $[V_{10}O_{28}]^{6-}$ has been reported in many articles with almost the same structures [25, 27, 29, 30, 32]. The differences of these decavanadates are the counter cations and the solvent molecules. For example, counter cations and solvent in decavanadate $[NH_4]_2[Mn(salen)(H_2O)_2]_4[V_{10}O_{28}]\cdot 6H_2O$ are $[NH_4]^+$, $[Mn(salen)(H_2O)_2]^+$, and H_2O [25]. The $[V_{10}O_{28}]^{6-}$ of **1** exhibits a cage-like structure, made up of 10 edge-sharing VO_6 octahedra as illustrated in figure 1. Vanadium in $[V_{10}O_{28}]^{6-}$ are distorted octahedral. There are six vanadiums in the equatorial plane and two above and two below the plane. Oxygens in $[V_{10}O_{28}]^{6-}$ can be divided into four different types: terminal (O(9), O(10), O(12), O(14)), μ_2 (O(1), O(5), O(6), O(7), O(8), O(11), O(13)), μ_3 (O(2), O(4)), and μ_6 (O(3)). The bond lengths of V–O are 1.595(4)–1.608(4) Å for terminal, 1.680(4)–2.054(4) Å for μ_2–O, 1.906(4)–2.038(4) Å for μ_3–O and 2.108(4)–2.325(4) Å for μ_6–O. The O–V–O angles range from 74.08(14)° to 174.9(2)°, consistent with previously reported $[V_{10}O_{28}]^{6-}$ clusters [25–32]. In $[Co(pyim)_3]^{3+}$, Co^{3+} is coordinated by six nitrogens from three 2-(2-pyridyl)-imidazole molecules to form a $[CoN_6]$ octahedral structure. The Co–N bond lengths are 1.890(5)–1.948(5) Å. Waters disperse around $[Co(pyim)_3]^{3+}$ and $[V_{10}O_{28}]^{6-}$. Compound **1** has a 3-D supramolecular structure assembled through extensive hydrogen–bonding interactions, O–H···O, and N–H···O, with the O···O and O···N distances in the range 2.65(2)–3.266(11) Å and 2.658(6)–2.962(12) Å (table S3). The waters have very strong hydrogen bonding interactions with each other to form two types of water clusters: $(H_2O)_6$ and $(H_2O)_2$ in **1**, with average O···O distance of 2.759–2.817 Å (figure 2). The water clusters in **1** are reminiscent of other hydrate-supramolecular aggregates [39, 40]. There are some disorders

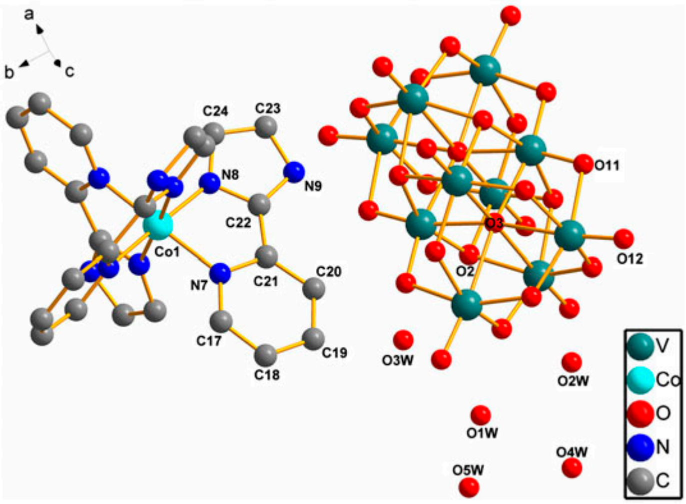

Figure 1. The structures of $[Co(pyim)_3]_2[V_{10}O_{28}]\cdot 7H_2O$ with atom-labeling schemes (hydrogens are omitted for clarity).

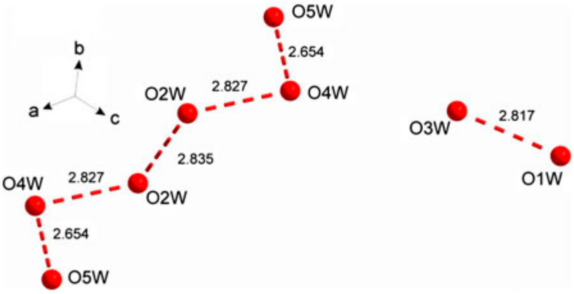

Figure 2. The $(H_2O)_6$ water cluster and $(H_2O)_2$ water cluster in **1**.

for O3w, O4w, and O5w with occupancy factors being 0.5, 0.5, and 0.5, respectively. $[V_{10}O_{28}]^{6-}$ clusters are linked by $(H_2O)_2$ water clusters via O1w–H· · ·O9, O3w–H· · ·O1, and O3w–H· · ·O2 hydrogen bonds to form a 1-D chain (figure 3). Adjacent 1-D chains are linked by O2w and its crystallographic partners of the $(H_2O)_6$ water clusters using hydrogen bonds to make a 2-D H_2O–$[V_{10}O_{28}]^{6-}$ soft layer, which is shown in figure 4. $[Co(pyim)_3]^{3+}$ are inserted between adjacent layers, while H_2O–$[V_{10}O_{28}]^{6-}$ layers are further connected by $[Co(pyim)_3]^{3+}$ using N9–H· · ·O4 and N6–H· · ·O13 hydrogen bonds to generate a 3-D supermolecular open framework, as depicted in figure 5.

The oxidation state for Co in **1** is calculated based on bond valence sum calculations [41]. The calculations indicate that Co is +3.25, confirming oxidation state +3 for Co ion, and in agreement with the formula of **1**.

Replacing $Co(CH_3CO_2)_2{\cdot}4H_2O$ by $Ni(CH_3CO_2)_2{\cdot}4H_2O$, we got **2**, whose structure is quite different from **1**. Compared to **1**, the cations of **2** are $[Ni(pyim)_3]^{2+}$. Due to the inversion center, protonation at O(9) generates diprotonated decavanadate unit $[H_2V_{10}O_{28}]^{4-}$ (figure 6). A hydrogen was clearly found from the difference map and the O(9)–H(9) bond distance is 0.804(9) Å. The Ni–N distances vary from 2.045(3) to 2.151(3) Å. The V–O distances vary from 1.595(2) to 2.365(2) Å. The O–V–O angles are 73.71(8)°–174.18(11)°. Distances and angles of the hydrogen bonds in **2** are listed in table S4. There is only one type of $(H_2O)_2$ water cluster in **2** (figure 6); $(H_2O)_2$ water clusters link $[H_2V_{10}O_{28}]^{4-}$ anions to form a 2-D sheet structure, as shown in figure 7. O2w is a H-acceptor connecting O1w by hydrogen bonds with O· · ·O distance of 2.681) Å, and then $(H_2O)_2$ clusters connect three adjacent $[H_2V_{10}O_{28}]^{4-}$ anions to form a $\{[H_2V_{10}O_{28}]\cdots(H_2O)_2\}_n$ layer. There are $[Ni(pyim)_3]^{2+}$ cations between the inorganic layers. Adjacent 2-D layers are connected by N–H· · ·O hydrogen bonds to make a 3-D supermolecular open framework (figure 8).

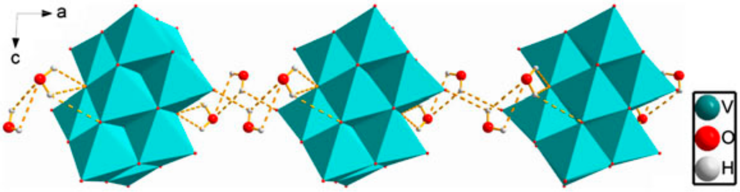

Figure 3. The 1-D chain constructed by $[V_{10}O_{28}]^{6-}$ anions and $(H_2O)_2$. (The decavanadate anions are represented in aqua polyhedron mode.)

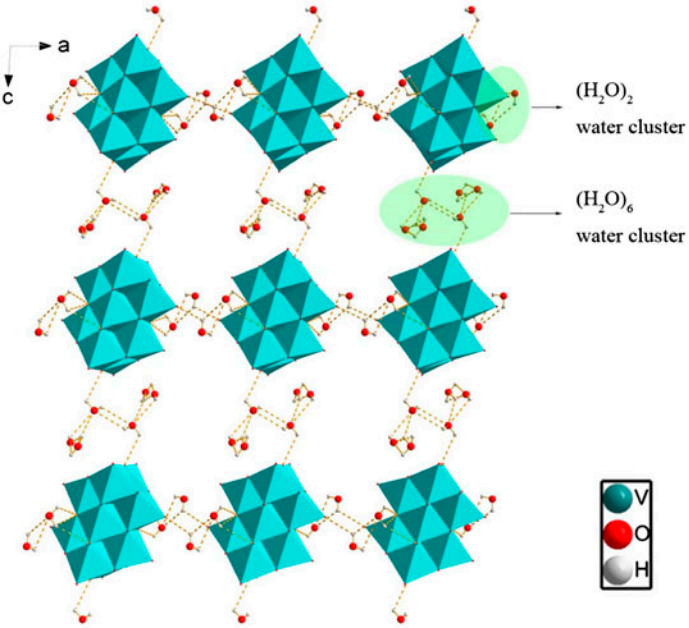

Figure 4. The 2-D layer constructed by $[V_{10}O_{28}]^{6-}$ and water viewing along the *b*-axis.

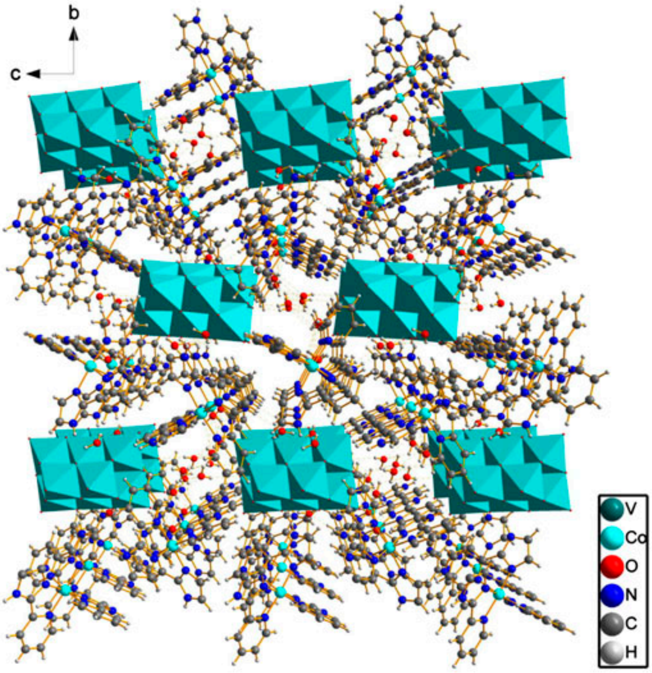

Figure 5. $[Co(pyim)_3]^{3+}$ filled between adjacent polyanion layers by hydrogen bonds to make a 3-D framework.

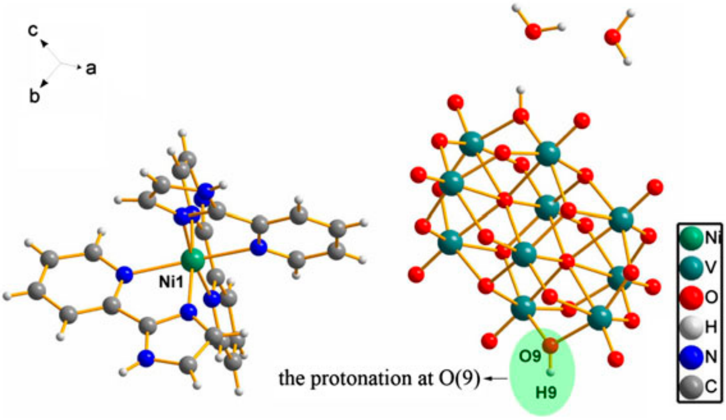

Figure 6. The structure of $[Ni(pyim)_3]_2[H_2V_{10}O_{28}]\cdot 4H_2O$ with the atom-labeling schemes.

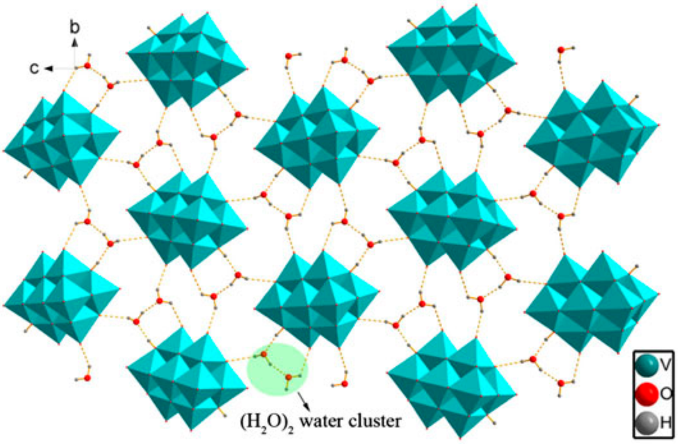

Figure 7. The structure of inorganic layer in **2** viewing along the *a*-axis.

Assignment of oxidation states for V of **1** and **2** are calculated based on bond valence sum calculations [42]. The calculations indicate +5 V in both **1** and **2**.

3.3. *IR spectrum*

IR spectra of **1** and **2** are shown in figure S1. The strong band at $960\,cm^{-1}$ is due to ν(V=O); bands at $580–840\,cm^{-1}$ are attributed to ν(O–V–O) and ν(V–O_b). Typically sharp peaks for 2-(2-pyridyl)-imidazole are $1100–1620\,cm^{-1}$. In addition, bands at $3400\,cm^{-1}$ are due to ν(O–H).

3.4. *PXRD analysis*

PXRD measurements for **1** and **2** were determined at room temperature. As shown in figures S2a and S2b, the peak positions of the experimental and simulated XRD patterns of **1** and **2** are in agreement, indicating the phase purity of **1** and **2**.

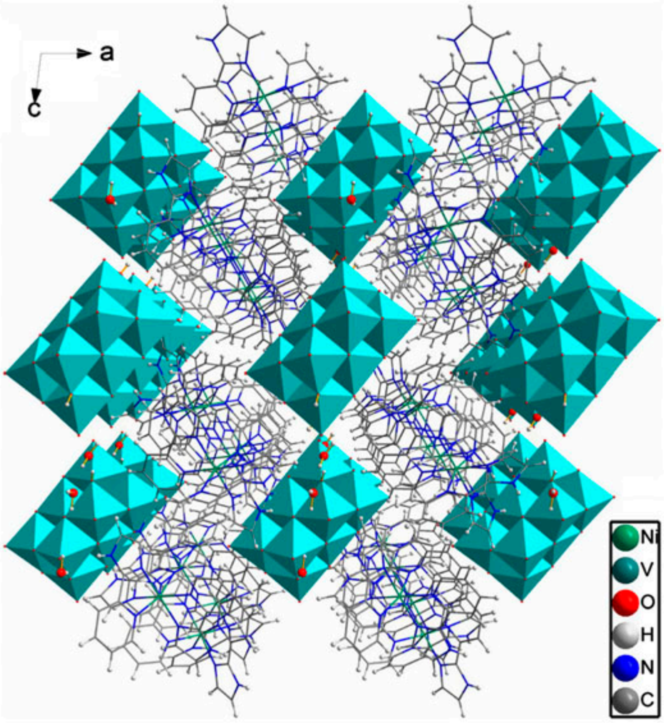

Figure 8. The supermolecular framework of **2**.

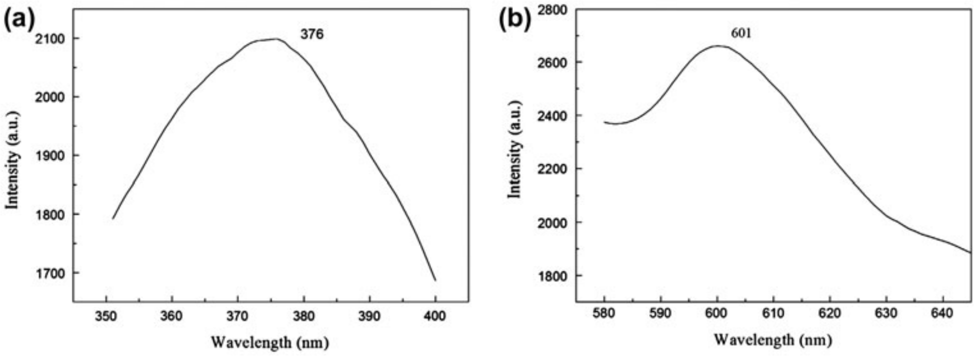

Figure 9. Excitation (a) and emission (b) spectra of **2**.

3.5. *Thermal analysis*

Thermal analyses of **1** and **2** were performed from 25 to 800 °C. As shown in figure S3a, weight loss of 5.98% from 25 to 310 °C corresponds to the removal of H_2O (Calcd 6.09%). Weight loss of 41.51% from 310 to 800 °C can be attributed to decomposition of pyim (Calcd 41.97%).

Total weight loss of **2** (figure S3b) from 25 to 800 °C is 46.56% (Calcd 46.69%), due to removal of H_2O and pyim.

3.6. *Fluorescence spectrum*

The fluorescence spectra of **2** were recorded in solid at room temperature. The maximum excitation and emission wavelengths of **2** are 376 and 601 nm, as shown in figure 9. Fluorescence of **2** is attributed to $[Ni(pyim)_3]^{2+}$. The maximum emission of **2** has a red shift compared to pyim (370 nm) [43]. It can be assigned to π–π^* fluorescence and the ligand-to-metal charge transfer. The enhanced fluorescence efficiency of **2** is due to coordination of pyim, which reduces the energy loss by radiationless thermal vibrations. Fluorescence of **1** is not observed, due to fluorescence quenching.

4. Conclusions

Two new decavanadate metal compounds based on $[V_{10}O_{28}]^{6-}$ and pyridyl imidazole $[Co(pyim)_3]_2[V_{10}O_{28}]\cdot 7H_2O$ (**1**) and $[Ni(pyim)_3]_2[H_2V_{10}O_{28}]\cdot 4H_2O$ (**2**) are synthesized under solvothermal condition. Although pyim was used as ligand in **1** and **2**, the V–O cluster anions are different. The structural analysis of both the compounds demonstrate transition metal complexes acted as balance cations and play an important role in formation of M–O cluster anions.

Supplementary material

CCDC 922345 and 922346 for **1** and **2** contain the supplementary crystallographic data. The date can be obtained free of charge via http://www.ccdc.com.ac.uk/conts/retrieving.html, or from Cambridge Crystallographic Data Center, 12 Union Road, Cambridge CB2 1E2, UK; Fax: +44 1223 336 033; or Email: deposit@ccdc.cam.ac.uk.

Acknowledgments

We gratefully acknowledge the Natural Science Foundation of Jiangsu Province (Grant BK2012823), and the doctoral program Foundation of Ministry of Education (20103221120002) for financial support.

References

[1] K. Fukaya, T. Yamase. *Angew. Chem. Int. Ed.*, **42**, 654 (2003).
[2] S.T. Zheng, J. Zhang, J.Q. Xu, G.Y. Yang. *J. Solid State Chem.*, **178**, 3740 (2005).
[3] C.P. Pradeep, D.L. Long, C. Streb, L. Cronin. *J. Am. Chem. Soc.*, **130**, 14946 (2008).
[4] C.L. Hill, C.M. Prosser-McCartha. *Coord. Chem. Rev.*, **143**, 407 (1995).
[5] J.T. Rhule, C.L. Hill, D.A. Judd, R.F. Schinazi. *Chem. Rev.*, **98**, 327 (1998).
[6] D.E. Katsoulis. *Chem. Rev.*, **98**, 359 (1998).
[7] E. Coronado, C.J. Gomez-Garcia. *Chem. Rev.*, **98**, 273 (1998).
[8] D.L. Long, E. Burkholder, L. Cronin. *Chem. Soc. Rev.*, **36**, 105 (2007).
[9] D. Hagrman, C. Zubieta, D.J. Rose, J. Zubieta, R.C. Haushalter. *Angew. Chem. Int. Ed. Engl.*, **36**, 873 (1997).

[10] D. Hagrman, P.J. Hagrman, J. Zubieta. *Angew. Chem. Int. Ed.*, **38**, 3165 (1999).
[11] M.I. Khan, E. Yohannes, V.O. Golub, C.J. O'Connor, R.J. Doedens. *Chem. Mater.*, **19**, 4890 (2007).
[12] R.F. Luis, M.K. Urtiaga, J.L. Mesa, K. Vidal, L. Lezama, T. Rojo, M.I. Arriortua. *Chem. Mater.*, **22**, 5543 (2010).
[13] A. Muller, F. Peters, M.T. Pope, D. Gatteschi. *Chem. Rev.*, **98**, 239 (1998).
[14] J. Livage. *Coord. Chem. Rev.*, **178**, 999 (1998).
[15] C. Wang, Z. Zhang, J. Fu, Y. Xu, D. Zhu. *Chem. Eur. J.*, **18**, 11909 (2012).
[16] V.W. Day, W.G. Klemperer, O.M. Yaghi. *J. Am. Chem. Soc.*, **111**, 4518 (1989).
[17] A. Bino, S. Cohen, C. Heitner-Wirguin. *Inorg. Chem.*, **21**, 431 (1982).
[18] H.T. Evans. *Inorg. Chem.*, **5**, 967 (1966).
[19] V.W. Day, W.G. Klemperer, O.M. Yaghi. *J. Am. Chem. Soc.*, **111**, 5959 (1989).
[20] D. Hou, K.S. Hagen, C.L. Hill. *J. Am. Chem. Soc.*, **114**, 5864 (1992).
[21] G.K. Johnson, E.O. Schlemper. *J. Am. Chem. Soc.*, **100**, 3645 (1978).
[22] Y. Xu, G.P. Zhou, D.R. Zhu. *Inorg. Chem.*, **47**, 567 (2008).
[23] M.I. Khan, E. Yohannes, R.J. Doedens. *Angew. Chem. Int. Ed.*, **38**, 1292 (1999).
[24] Y. Xu, L.B. Nie, D.R. Zhu, Y. Song, G.P. Zhou, W.S. You. *Cryst. Growth Des.*, **7**, 925 (2007).
[25] S.W. Lin, Q. Wu, H.Q. Tan, E.B. Wang. *J. Coord. Chem.*, **64**, 3661 (2011).
[26] L. Klistincova, E. Rakovsky, P. Schwendt. *Inorg. Chem. Commun.*, **11**, 1140 (2008).
[27] J. Thomas, M. Agarwal, A. Ramanan, N. Chernova, M.S. Whittingham. *CrystEngComm.*, **11**, 625 (2009).
[28] T. McGlone, J. Thiel, C. Streb, D.L. Long, L. Cronin. *Chem. Commun.*, **48**, 359 (2012).
[29] W.T. Xu, F.L. Jiang, Y.F. Zhou, K.C. Xiong, L. Chen, M. Yang, R. Feng, M.C. Hong. *Dalton Trans.*, **41**, 7737 (2012).
[30] L. Jouffret, M. Rivenet, F. Abraham. *Inorg. Chem. Commun.*, **13**, 5 (2010).
[31] T. Kojima, M.R. Antonio, T. Ozeki. *J. Am. Chem. Soc.*, **133**, 7248 (2011).
[32] L. Klistincova, E. Rakovsky, P. Schwendt, G. Plesch, R. Gyepes. *Inorg. Chem. Commun.*, **13**, 1275 (2010).
[33] Y. Hayashi. *Coord. Chem. Rev.*, **255**, 2270 (2011).
[34] G.Z. Kaziev, A.V. Oreshkina, S.H. Quinones, A.F. Stepnova, V.E. Zavodnik, I. Antonio, D.A. Alekseev. *Russ. J. Coord. Chem.*, **36**, 887 (2010).
[35] C.L. Wang, J. Fu, H. Mei, D.W. Yan, Y. Chin. *J. Inorg. Chem.*, **28**, 176 (2012).
[36] O.V. Yakubovich, E.N. Ananeva, O.V. Dimitrova, V.S. Urusov. *Dokl. Phys.*, **47**, 346 (2002).
[37] B. Chiswell, F. Lions, B. Morris. *Inorg. Chem.*, **3**, 110 (1964).
[38] G.M. Sheldrick. *SHELXTL (Version 5.10)*, *Bruker AXS Inc.*, Madsion, WI (1997).
[39] M.L. Wei, C.Y. Duan, Q.J. Meng. *J. Am. Chem. Soc.*, **128**, 13318 (2006).
[40] C.Y. Duan, D. Guo, Q.J. Meng. *J. Am. Chem. Soc.*, **132**, 3321 (2010).
[41] I.D. Brown, D. Altermatt. *Acta Cryst.*, **B41**, 244 (1985).
[42] I.D. Brown. *Chem. Rev.*, **109**, 6858 (2009).
[43] S.M. Yue, N. Li, J.Y. Bian, T.T. Hou, J.F. Ma. *Synth. Met.*, **162**, 247 (2012).